Molecular Crystals and Liquid Crystals Science and Technology. Section A. Molecular Crystals and Liquid Crystals
Publication details, including instructions for authors and subscription information:
http://www.tandfonline.com/loi/gmcl19

# Computational Modelling Study of the Growth Morphology of the Normal Alkane Docosane and Its Mediation by "Tailor-Made" Additives

G Clydesdale [a] , K J Roberts [a b] & K. Lewtas [c]

[a] Department of Pure and Applied Chemistry, University of Strathclyde, Glasgow, G1 1XL, Scotland, U.K.

[b] SERC Laboratory, Daresbury, Warrington, WA4 4AD, UK

[c] Exxon Chemical Ltd, Milton Hill, Abingdon, Oxfordshire, OX13 6BB, England, U.K.

Version of record first published: 24 Sep 2006.

To cite this article: G Clydesdale , K J Roberts & K. Lewtas (1994): Computational Modelling Study of the Growth Morphology of the Normal Alkane Docosane and Its Mediation by "Tailor-Made" Additives, Molecular Crystals and Liquid Crystals Science and Technology. Section A. Molecular Crystals and Liquid Crystals, 248:1, 243-276

To link to this article: http://dx.doi.org/10.1080/10587259408027182

*Mol. Cryst. Liq. Cryst.* 1994, Vol. 248, pp. 243–276
Reprints available directly from the publisher
Photocopying permitted by license only

Printed in the United States of America



# COMPUTATIONAL MODELLING STUDY OF THE GROWTH MORPHOLOGY OF THE NORMAL ALKANE DOCOSANE AND ITS MEDIATION BY "TAILOR-MADE" ADDITIVES.

G CLYDESDALE AND K J ROBERTS+
Department of Pure and Applied Chemistry,
University of Strathclyde, Glasgow, G1 1XL, Scotland, U.K.

K. LEWTAS,
Exxon Chemical Ltd, Milton Hill, Abingdon, Oxfordshire OX13 6BB, England, U.K.

+ also at SERC Laboratory, Daresbury, Warrington, WA4 4AD, UK

Abtract A generalised approach for modelling the morphology of molecular crystals in the presence of "tailor-made" additives of both the disruptor and blocker types is presented and demonstrated by a consideration of the effects of a series of eight "tailor-made" additives on the morphology of the long chain normal alkane docosane ($C_{22}H_{46}$). The additives considered include n-alkane homologues of different chain lengths (both longer and shorter than the host) along with methyl- substituted n-alkanes.

Considering other n-alkane homologues as additives demonstrates the ability of these materials to incorporate easily into docosane crystals although the habit-modifying properties are not great due to the similarity with the host sytem and the anisotropic nature of the bonding. The predicted crystals are thinner along the c-direction compared to the pure system, although they increase in thickness with chain length from n=20-24. It is shown that addition of methyl groups to n-alkanes can have a significant effect on their morphology forming more equant crystals as the number of methyl groups is increased. The asymmetry of the additives greatly affects the relative growth rates of pairs of faces (hkl) and (-h-k-l) leading to a polar morphology.

## INTRODUCTION

The ability to predict crystal morphology with and without the presence of habit-modifying additives is of great use in allowing the optimisation of growth conditions

modifying additives is of great use in allowing the optimisation of growth conditions to produce a required crystal habit. Early studies[1-3] demonstrated that crystal morphology is related to crystal lattice symmetry, whilst later work[4-6] showed how the overall crystal morphology could be related to the interaction energies between crystallising units. Additive molecules affect the growth rate of crystal surfaces either by blocking the movement of surface step/kink terraces (referred to as blocking modifiers) or by incorporating in the solid-state and disrupting the intermolecular bonding networks (disrupting modifiers).

In previous papers[7,8] we described computational approaches that we have developed for the simulation of the crystal morphology of molecular materials when mediated by the presence of disruptor and blocking "tailor-made" additives. These approaches are utilised in this paper to study the habit modification of a model system based on the long chain normal alkane docosane ($C_{22}H_{46}$; hereafter, for convenience, n-alkanes ($C_nH_{2n+2}$) are referred to by the carbon number $C_n$ only). Such materials impact on many areas of science and technology (e.g. polymer technology, food science, petrochemicals, biological interfaces, colloids) and crystallise with a simple plate- like morphology due to strong interchain interactions along the a and b directions leading to fast growth, with weak head-to-tail interactions in the c direction (parallel to the long axis) resulting in slow growth (see Figure 1). Such a morphology makes the effect of any habit modification clear.

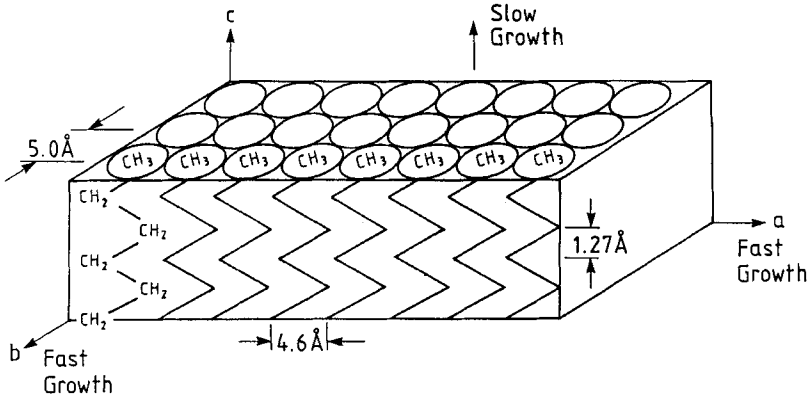


FIGURE 1 Schematic showing the growth of an n-alkane crystal. Close packed chains in the ab-plane lead to rapid growth in these directions, whilst weak head-to-tail interactions along the c-directions cause slow growth leading to a plate-like morphology dominated by {001) forms.

Firstly, other n-alkane homologues were considered as additives: two disruptor-type additives with smaller chain lengths ($C_{20}$ and $C_{21}$) and two blocker-type additives with longer chain lengths ($C_{23}$ and $C_{24}$). In each case there is an even numbered n-alkane homologue and an odd numbered homologue. The crystallisation of mixtures of n-alkanes is of importance as the close homologues are known to significantly incorporate on crystallisation[9,10] forming a solid- solution of even and odd chain lengths. The pure even and odd homologues crystallise in quite different systems (typically, triclinic and orthorhombic, respectively[11]) but both were chosen as additives to see if the even homologues would incorporate easier than the odd homologues due to the host system being that of an even homologue.

Secondly, simple methyl-substituted n-alkanes were considered as blocker-type additives to assess the effect of blocking certain crystal directions on morphology.

## BACKGROUND THEORY AND COMPUTATIONAL TECHNIQUES

### Modelling Crystal Morphology in the Absence of Growth Modifiers

Morphological modelling techniques are based upon correlating the bulk structure in some way with the crystal morphology. Solid-state calculations are used to determine the structural preference, in terms of (hkl), of a crystal growth layer (thickness $d_{hkl}$) to adsorb upon a growing crystal surface.

The geometrically-based Bravais-Friedel-Donnay-Harker (BFDH) approach[1-3] is used to identify likely growth forms while the energetic parameters defined by Hartman and Perdok[4,5] are used to allow morphological predictions. They defined the surface attachment energy ($E_{att}$) as the energy released on the addition of a growth slice to the surface of a growing crystal[6,12] and which is related to the crystallisation energy or lattice energy ($E_{cr}$) by:

$$E_{cr} = E_{sl} + E_{att} \quad (1)$$

where $E_{sl}$ is the intermolecular bonding energy contained within the surface growth slice. The growth rate of a given crystal face (hkl) is proportional to $E_{att}$ and hence inversely so to the morphological importance and $E_{sl}$[12]. The latter is thus a useful measure of the growth stability of a given crystal face. The assumption of the

proportionality of the growth rate and $E_{att}$ is only strictly valid for faces growing by a layer mechanism whereas we use it for all faces; such an approach, however, has been applied successfully to a variety of materials[6, 13-15].

Providing we assume that the relative intermolecular bond strengths as a function of (hkl) do not change significantly upon crystallisation we can calculate the lattice, slice and attachment energies from the bulk crystal structure[6] using the atom-atom method[16]. This is achieved by summing interactions between a central molecule and all the surrounding molecules (see Figure 2), where each intermolecular interaction is considered to be the sum of the constituent atom- atom interactions. For the work in this paper we use a Buckingham[17] potential with atom- atom parameters from Williams[18] to calculate the van der Waals interatomic energies. We omit the electrostatic contribution on the basis of previous work on long chain n-alkanes[19] which indicated it to be negligible.

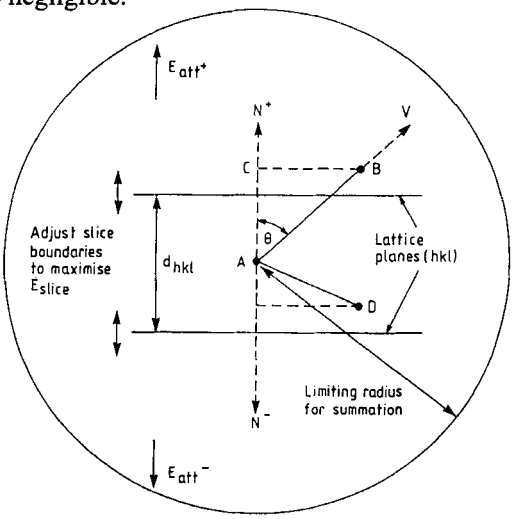


FIGURE 2 Basic approach for calculation of intermolecular interactions using the atom-atom method showing how the lattice energy is partitioned between the slice and attachment energies within a limiting sphere. A is the central molecule, B is a molecule outside the slice, D is a molecule inside the slice, $N^+$ is the growth normal to the planes (h k l), $N^-$ is the growth normal to the planes (-h-k-l ), AB and AD are bonding vectors, $d_{hkl}$ is the interplanar spacing, θ is the angle between the growth normal and the bonding vector and AC is the component of the vector AB parallel to N the growth normal. Note that the slice-boundaries defined by $d_{hkl}$ may be shifted along the growth normal to obtain the energetically most stable slice.

We can relate the lattice energy to the sublimation enthalpy to obtain an "experimental" lattice energy ($V_{exp}$) where:

$$V_{exp} = \Delta H_{sub} - 2RT \quad (2)$$

For our work we use the computer programs MORANG[20], HABIT[21] and CERIUS[22] to respectively determine the symmetry reduced growth slices according to BFDH rules, calculate $E_{att}$ using the atom-atom method and to plot the resulting crystal morphology using Wulff's method[23].

Assessing the Effects of Tailor-Made Additives

Tailor-made additives[24] are "designer" impurities which have enough molecular compatibility with the host system to be able to incorporate onto the surface of the growing crystal and modify the energetics by preventing oncoming molecules getting into their rightful positions at the surface. In order to model the change of growth rate as a function of additive we need to modify Hartman and Perdok's classical definition of attachment energy and introduce some new terms.

In a previous paper[7] we noted that the nature of the intermolecular potential calculation for a crystal lattice without additive ensures that the growth slice is apolar and that therefore $E_{att(+)}$ is equal to $E_{att(-)}$ (see Figure 2). However, the incorporation of an additive violates the local crystal symmetry and we have to calculate the modified values of these separately. Thus in order to fully assess the structural ramifications of the additive adsorption we need to calculate five additional terms in all: $E_{sl'}$, $E_{att(+)'}$, $E_{att(-)'}$, $E_{att(+)''}$ and $E_{att(-)''}$. These are illustrated in Figure 3. $E_{sl'}$ is the slice energy calculated with an additive at the centre of the slice[24]; $E_{att'}$ is the attachment energy of a growth slice containing an additive onto a pure surface[24] and $E_{att''}$ is the attachment energy of a pure growth slice onto a surface containing an additive. The computer program HABIT[21] has been extended[25] to allow calculation of these modified energy terms associated with the additive adsorption process. The computational procedure employed is given in detail elsewhere[7].

We can assess how easily an additve will adsorb onto a given crystal surface (hkl) by calculating the relative "binding or incorporation energy" ($\Delta b$), defined[6,24] as the difference between the incorporation energy of the additive ($E_{b'}$) and the pure material ($E_b$) where:

material ($E_b$) where:

$$\Delta b = E_{b'} - E_b = ( E_{sl'} + E_{att'} ) - ( E_{sl} + E_{att} ) \quad (3)$$

which we expand to give:

$$\Delta b = E_{b'} - E_b = ( E_{sl'} + E_{att(+)'} + E_{att(-)'} ) - ( E_{sl} + E_{att(+)} + E_{att(-)} ) \quad (4)$$

From this equation we can see that crystal faces where there is minimum change in the incorporation energy are where the additives are likely to incorporate. If $\Delta b$ is strongly dependant upon crystal orientation then the incorporation will be specific to one crystal face and vice-versa.

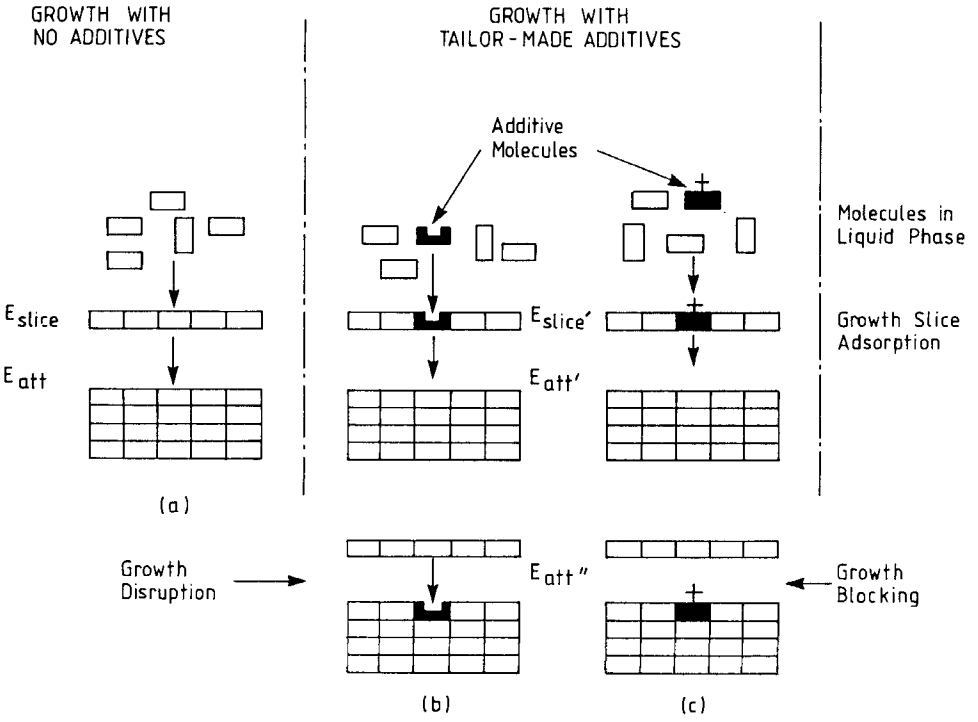


FIGURE 3 Schematic showing the definition of the energy terms $E_{att}$, $E_{att'}$, $E_{att''}$, $E_{sl}$ and $E_{sl'}$ used in morphological modelling for (a) pure systems and systems having (b) disruptive-type and (c) blocker-type tailor-made additives.

In our approach we propose the use of the further parameter $E_{att}''$ which reflects the energy released on the addition of a pure growth slice onto a surface on which an additive has adsorbed. This additional parameter can be used as a direct measure of the growth rate of a crystal face "poisoned" with a tailor-made additive molecule thus enabling calculation of the crystal morphology with an additive present.

In earlier work on the blocker type of additives, Docherty[26] commented on the need for an improved approach to obtain meaningful values for $E_{att}''$. Previously (e.g. refs. 24,26,27), blockers have been considered in the same way as disruptors thus giving rise to large, positive $E_{att}''$ values for faces where the blocking part of the additive hinders adsorbing molecules. These attachment energies with additive present cannot be utilised to produce a morphology but serve only as a guide of the "blocking ability" of the additive at each face.

Later[8] we improved our calculation of $E_{att}''$ by introducing vacancies in cases where the intermolecular interactions are unfavourable for steric reasons. This is achieved by calculating each intermolecular interaction and omitting its contribution to the energy terms if it is considered to result from the blocking nature of the additive[25] (for an illustration of this procedure see Figure 4). The steric repulsions are a result of atoms of the blocker residing close to, or actually in, the same physical space in the crystal as atoms of the adjacent host molecules. Effectively, then, removing an intermolecular interaction's contribution to the lattice energy is the same as omitting the molecule. This vacancy concept exhibits some of the main effects of blocker-type additives: a lowering in $E_{att}''$ (and hence an increase in morphological importance) and the loss of host molecules from adsorbing due to additive molecules blocking surface sites.

The modified $E_{att}''$ parameter may now be used to obtain a morphological representation of the effects of a blocker additive which was not previously possible. When there is a noticeable difference between $E_{att(+)}''$ and $E_{att(-)}''$ the former values should be used for faces (hkl) and the latter values used for faces (-h-k-l ). In this way the polar effect of the additive may be modelled. Such a morphology is indicated below as "model 2": "model 1" refers to morphologies predicted using $E_{att}''$ as a measure of growth rate for all faces; "model 3" is computed using a combination of $E_{att}$ and $E_{att}''$ values if this is thought more appropriate (such cases are detailed in the accompanying text).

In the examples given below, for both types of additive, the change in incorporation energy ($\Delta b$) is given for each form along with the host and additive

attachment energies. The host attachment energy ($E_{att}$) is the sum of $E_{att(+)}$ and $E_{att(-)}$ (which are essentially of equal magnitude), whilst $E_{att}''$ is the sum of $E_{att(+)}''$ and $E_{att(-)}''$ (which may differ in magnitude due to the asymmetry introduced by the additive). It may be noted that the $E_{att}''$ values are averaged over all symmetry-independent sites in the unit cell, whereas the $\Delta b$ values are site-specific. Note also that in all our definitions we halve all atom-atom interactions compared to refs. 6,24 (see Appendix A in ref. 7).

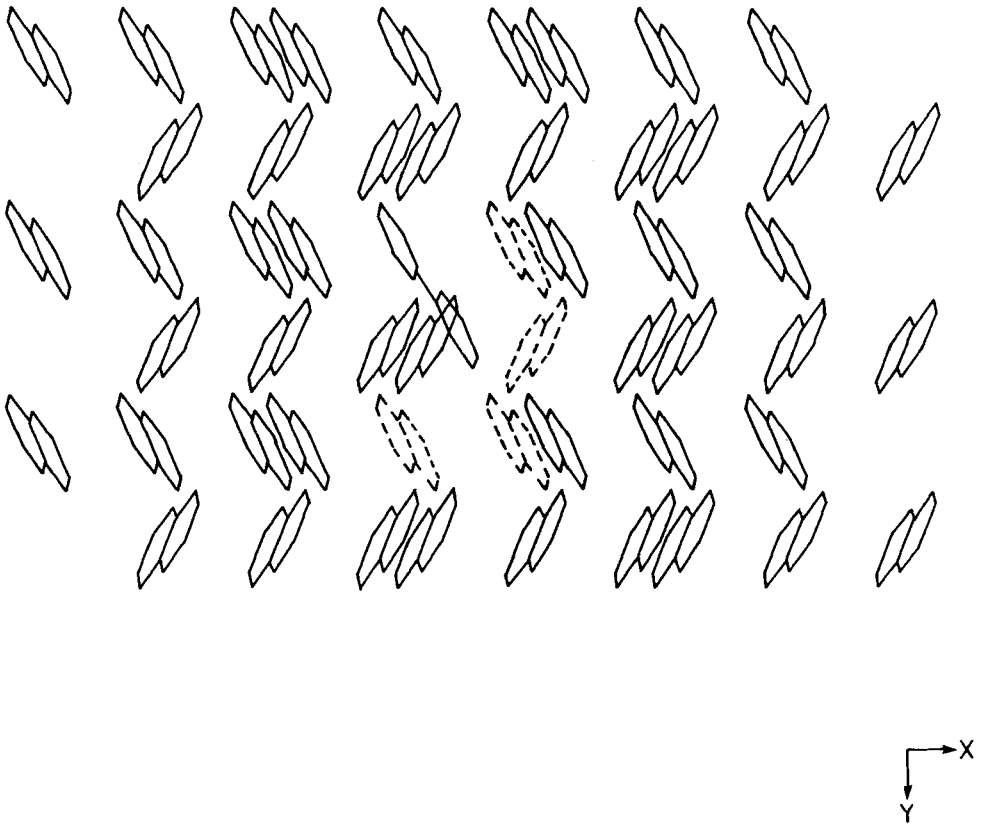


FIGURE 4 Example showing the blocking nature of a biphenyl additive molecule in a naphthalene crystal: (a) showing biphenyl blocking adjacent naphthalene molecules; (b) showing the inclusion of vacancies for unfavourable steric intermolecular interactions.

As part of this procedure we also estimate the un-relaxed vacancy formation energy ($E_v$):

$$E_v = E_{cr} - \left( \sum_{i=1}^{N_m} \sum_{j=1}^{Z} E_{vac}(ij)/Z.N_m \right) \quad (5)$$

where $E_{vac}$ is the lattice energy calculated with a vacancy placed at the molecular site (i) within the number of molecules ($N_m$) defined by the van der Waals cut-off radius ($R_{lim}$) of the atom- atom summation and averaged over $N_m$ and all symmetry-independent sites in the unit cell (j). The number of vacancies ($N_v$) generated by each blocking additive is also given here. Both $E_v$ and $N_v$ provide an additional benchmark as to the likelihood, on an energetic basis, of additive incorporation.

Since the molecular structures for the additive molecules studied here were not available from the CSSR X-ray database[28] they were constructed and minimised using the molecular graphics packages CHEM-X[29] and INTERCHEM[30]. For docosane the crystal packing in the triclinic (space group P-1) lattice was then optimised via the program PCK83[16] using the cell parameters predicted by Nyburg and Potworowski[31]: a=4.285Å, b=4.820Å c=27.43Å; α=85.66°, β=68.16°, γ=72.70° after fitting the minimised molecular structure to the known isotypic structure of $C_{18}$[32] to determine the correct orientation. Coordinates for the various additive molecules in terms of the docosane lattice were obtained by fitting the addditve to the host at one of the end methyl groups and the new parameters described above for predicting the morphology with the presence of an additive calculated.

## THE MORPHOLOGY OF DOCOSANE

Docosane crystallises in the triclinic space group P-1 with one molecule in the unit cell. The calculated lattice energy of -41.90 kcal/mol ($R_{lim}$=30Å, $N_m$=264) can be compared to the "experimental" lattice energy for n-octadecane ($C_{18}$) of -37.78 kcal/mol from the known sublimation enthalpy of 36.73 ±1.20 kcal/mol[33]). The results of the morphological predictions are given in Table 4; the corresponding attachment energy model of the crystal is shown in Figure 5. The predicted morphology reflects the expected plate-like habit[34,35] and is dominated by {001}

and bounded by smaller {010}, {102} and {103} faces. (Other possible (hk0) faces such as (100), (010) and (110) were not included in the energy calculations as the selection process of the BFDH rules did not indicate them to be significant.)

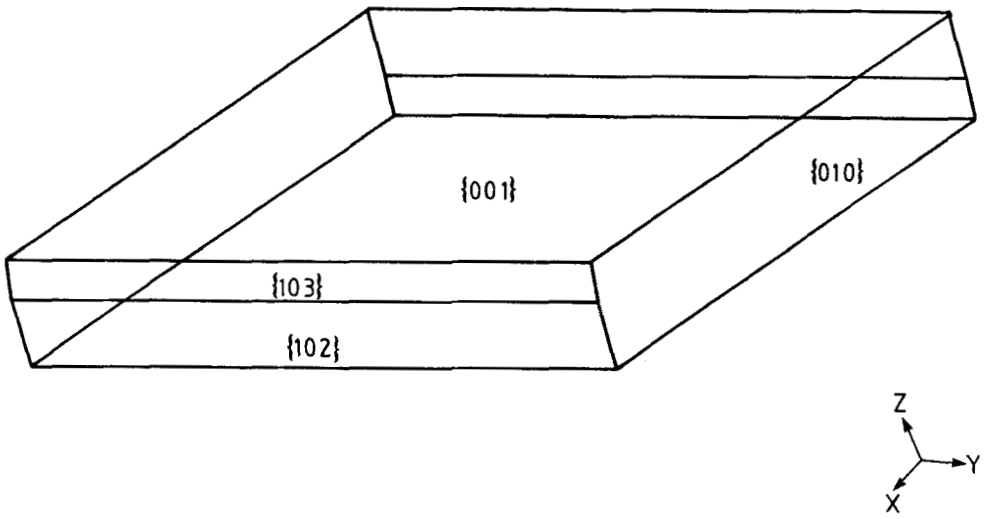


FIGURE 5 Attachment energy morphology of docosane ($C_{22}$).

## THE EFFECT OF CLOSE HOMOLOGUES ON THE MORPHOLOGY OF DOCOSANE

This section considers the habit-modification of docosane by other similar n-alkane homologues. These are divided into two types by their chain lengths: those shorter than docosane ($C_{20}$ and $C_{21}$) are considered as disruptor-type additives; those with longer chain lengths ($C_{23}$ and $C_{24}$) are considered as blocker-type additives. Since the additive molecules are so similar to the host a large change in the morphology is not likely. Additive molecules have most effect when they interrupt a chain of strong-bonding e.g. hydrogen-bonds in benzamide/benzoic acid[6,8]. In the cases considered in this paper the bonding is anisotropic and the effect of the additives is likely to be less specific.

Tables 1-3 summarise the morphological impact of the additives (Figures 6-8) by listing the surface area of the habit faces along with aspect ratios for both the host system and the habit- modified crystals.

TABLE 1 Surface areas (as percentage of the total surface area) in units$^2$ for model 1 (standard) morphologies of docosane ($C_{22}$, "host") with eight different additives. "Total" denotes the total surface area, "A.R." the aspect ratio.

| (h k l) | Host | $C_{20}$ | $C_{21}$ | $C_{23}$ | $C_{24}$ | ADDT1 | ADDT2 | ADDT3 | ADDT4 |
|---|---|---|---|---|---|---|---|---|---|
| 0 0 1 | 78.40 | 83.91 | 81.71 | 81.92 | 80.14 | 73.71 | 73.71 | 70.90 | 69.36 |
| 0 1 0 | 11.89 | 8.81 | 10.05 | 9.07 | 7.97 | 10.22 | 14.31 | 11.70 | 13.45 |
| 0 1 1 | 0.00 | 0.00 | 0.00 | 0.79 | 2.87 | 2.12 | 0.00 | 4.36 | 3.48 |
| 1 0 3 | 3.62 | 2.86 | 3.10 | 2.22 | 2.21 | 3.25 | 4.20 | 3.06 | 3.31 |
| 1 0 2 | 6.08 | 4.42 | 5.14 | 6.00 | 6.81 | 10.70 | 7.78 | 9.97 | 10.39 |
| Total: | 7569.13 | 5820.20 | 6580.78 | 7318.69 | 7837.76 | 4427.29 | 4817.69 | 3538.21 | 3636.67 |
| A.R. | 12.53 | 17.93 | 15.39 | 15.60 | 13.98 | 9.68 | 9.66 | 8.53 | 7.93 |

TABLE 2 Surface areas (as percentage of the total surface area) in units$^2$ for model 2 (polar) morphologies of docosane ($C_{22}$, "host") with eight different additives. "Total" denotes the total surface area, "A.R." the aspect ratio. * for $C_{23}$ and $C_{24}$ this face is (0-11).

| (h k l) | Host | $C_{20}$ | $C_{21}$ | $C_{23}$ | $C_{24}$ | ADDT1 | ADDT2 | ADDT3 | ADDT4 |
|---|---|---|---|---|---|---|---|---|---|
| 0 0 1 | 39.20 | 41.66 | 40.81 | 40.63 | 39.81 | 36.96 | 36.87 | 35.58 | 34.90 |
| 0 0-1 | 39.20 | 42.13 | 40.86 | 41.16 | 40.29 | 36.74 | 36.83 | 35.34 | 34.45 |
| 0 1 0 | 5.95 | 0.67 | 4.12 | 0.74 | 1.42 | 6.15 | 7.16 | 7.22 | 8.44 |
| 0-1 0 | 5.95 | 4.43 | 5.03 | 4.36 | 4.86 | 3.42 | 7.16 | 4.47 | 4.23 |
| 0 1 1 | 0.00 | 3.84 | 0.92 | 4.30 | 4.07 | 0.00 | 0.00 | 0.78 | 0.00 |
| 0-1-1* | 0.00 | 0.00 | 0.00 | 0.60 | 0.54 | 2.79 | 0.00 | 3.58 | 4.30 |
| 1 0 3 | 1.81 | 0.90 | 1.21 | 0.21 | 0.19 | 2.42 | 1.96 | 2.28 | 2.49 |
| -1 0-3 | 1.81 | 1.96 | 1.90 | 2.02 | 2.02 | 0.83 | 2.25 | 0.79 | 0.82 |
| 1 0 2 | 3.04 | 2.74 | 2.92 | 3.90 | 4.31 | 4.55 | 4.03 | 4.23 | 4.35 |
| -1 0-2 | 3.04 | 1.68 | 2.22 | 2.09 | 2.47 | 6.14 | 3.74 | 5.72 | 6.03 |
| Total: | 7569.13 | 1446.53 | 1643.00 | 1817.77 | 1953.52 | 1105.45 | 1204.42 | 884.37 | 907.66 |
| A.R. | 12.53 | 43.97 | 21.95 | 20.66 | 15.26 | 12.11 | 12.76 | 12.33 | 12.29 |

TABLE 3 Surface areas (as percentage of the total surface area) in units$^2$ for model 3 (additional) morphologies of docosane ($C_{22}$, "host") with Additives 1-4. "Total" denotes the total surface area, "A.R." the aspect ratio.

| (h k l) | Host | ADDT1 | ADDT2 | ADDT3 | ADDT4 |
|---|---|---|---|---|---|
| 0 0 1 | 78.40 | 72.87 | 78.36 | 70.07 | 70.19 |
| 0 1 0 | 11.89 | 10.37 | 11.91 | 11.89 | 13.28 |
| 0 1 1 | 0.00 | 2.36 | 0.00 | 4.63 | 3.20 |
| 1 0 3 | 3.62 | 3.51 | 3.63 | 3.29 | 3.09 |
| 1 0 2 | 6.08 | 10.89 | 6.09 | 10.12 | 10.25 |
| Total: | 7569.13 | 4472.80 | 7572.84 | 3575.96 | 3598.43 |
| A.R. | 12.53 | 9.28 | 12.50 | 8.21 | 8.24 |

Disruptor-Type Additives: Docosane with Eicosane as an Additive

Firstly, eicosane ($C_{20}$) was introduced as an additive and the modified slice and attachment energies computed (see Table 4). The effect of the additive on the morphology is shown in Figure 6(b). The overall morphology is very similar to the pure system (Figure 6(a)) except that the aspect ratio of the crystals is increased upon the addition of additive.

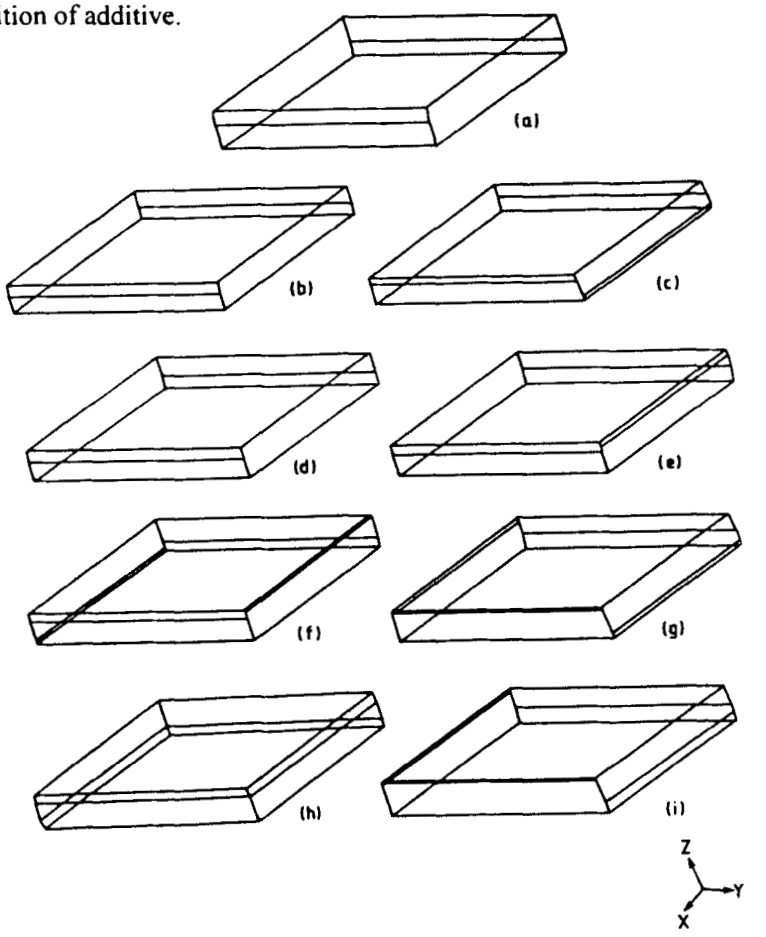


FIGURE 6 Habit modification of docosane by close n-alkane homologues: (a) attachment energy morphology of docosane; (b) with eicosane ($C_{20}$) additive (model 1); (c) with eicosane additive (model 2); (d) with heneicosane ($C_{21}$) (model 1); (e) with heneicosane (model 2); (f) with tricosane ($C_{23}$) (model 1); (g) with tricosane (model 2); (h) with tetracosane (model 1); (i) with tetracosane (model 2). Faces additional to those shown in Figure 5 are {011}.

From the incorporation energy results (see Table 4) it can be seen that eicosane molecules can fit easily in {001} faces as the interactions at these faces is simply between end methyl groups - there is little difference here between docosane and eicosane molecules. There is little loss of incorporation energy for all faces indicating that eicosane molecules are easily accomodated due to the similarity of the host and additive molecules, the loss in energy being due to the shorter chain length of the additive. The increase in the aspect ratio presumably reflects the fact that the shorter eicosane molecule reduces the (001) attachment energy contribution by reducing the effect of methyl-methyl interactions across the (001) basal plane. These results are in good agreement with observations of n-alkane crystallised from solution[34,35] which in general have much larger aspect ratios than those observed when crystallised by sublimation[36].

The intermolecular bonding results given in Table 5 further demonstrate the effect of the additive in the c-direction: the [00-1] interaction decreases from -0.24 kcal/mol to only -0.04 with the additive present. This decreases the growth of the (001) face and increases the aspect ratio.

Since, in this case, the values for $E_{att(+)}''$ and $E_{att(-)}''$ are significantly different (see Table 4) a second model of the morphology was computed, shown in Figure 6(c). This polar crystal contains {011} forms but has no corresponding {0-1-1} forms.

TABLE 4 Changes in incorporation energy (Δb) and attachment energies for docosane with eicosane additive (in kcal/mol).

| FACE (hkl) | Δb | $E_{att(+)}''$ | $E_{att(-)}''$ | $E_{att}''$ | $E_{att}$ |
|---|---|---|---|---|---|
| (0 0 1) | 2.50 | -0.48 | -1.81 | -2.30 | -3.63 |
| (0 1 0) | 2.15 | -11.21 | -10.72 | -21.93 | -24.04 |
| (0 1 -1) | 1.57 | -12.01 | -10.78 | -22.80 | -25.49 |
| (0 1 1) | 2.02 | -10.74 | -11.44 | -22.18 | -24.42 |
| (0 1 -2) | 1.50 | -12.13 | -10.81 | -22.94 | -25.70 |
| (0 1 2) | 1.53 | -10.81 | -12.08 | -22.89 | -25.62 |
| (0 1 -3) | 1.49 | -12.15 | -10.82 | -22.97 | -25.74 |
| (1 0 3) | 1.46 | -12.49 | -14.23 | -26.72 | -29.73 |
| (1 0 2) | 1.53 | -12.46 | -14.10 | -26.56 | -29.49 |
| (0 1 3) | 1.50 | -10.83 | -12.14 | -22.97 | -25.73 |

TABLE 5 Intermolecular bonding analysis for docosane with eicosane additive. Bonds are between a central molecule [000] and a second molecule moved by [UVW] where U, V, W are multiples of the unit cell along the a, b and c-directions, respectively; bond energies are in kcal/mol.

| Bond | U | V | W | Bond Energy Host | Additive |
|---|---|---|---|---|---|
| a | 1 | 0 | 0 | -7.69 | -7.06 |
| b | -1 | 0 | 0 | -7.69 | -7.31 |
| c | 0 | -1 | 0 | -5.87 | -5.52 |
| d | 0 | 1 | 0 | -5.87 | -5.43 |
| e | -1 | 1 | 0 | -3.24 | -3.09 |
| f | 1 | -1 | 0 | -3.24 | -3.00 |
| g | 0 | 0 | 1 | -0.24 | -0.04 |
| h | 0 | 0 | -1 | -0.24 | -0.24 |

Disruptor-Type Additives: Docosane With Heneicosane As An Additive

The odd carbon-numbered n-alkane heneicosane ($C_{21}$) was also considered as a disruptor additive. This molecule possesses different symmetrical properties from docosane - it has a mirror plane about the central carbon atom compared to the centre of inversion possessed by the even- numbered n-alkanes. This may cause it to incorporate in a different manner from eicosane as the end methyl groups will be in less energetically favourable packing positions.

The results of the attachment energy calculations with $C_{21}$ present are given in Table 6 and the two computed morphologies (models 1 and 2) in Figures 6(d) and 6(e) (compare with Figure 6(a) which is the attachment energy model of pure docosane). The lower incorporation energy values for heneicosane compared to those obtained for eicosane are probably simply due to the increased intermolecular interactions contributed by the longer chain. The odd n-alkane seems to accomodate just as effectively as the even homologue.

The model 1 morphology (Figure 6(d)) exhibits a very similar habit to the host system containing the same forms but with a slightly smaller aspect ratio indicating a thicker crystal. The model 2 morphology (Figure 6(e)) bears a close comparison with the model 2 morphology of the eicosane/docosane system. The main difference here relates to the side faces: {011} forms are favoured over the competing {01-1} forms with $C_{21}$ as the additive. Table 6 demonstrates the expected disparity between the positive and negative attachment energies with the main difference being along the c-direction. Here the difference is not as great as with eicosane additive due to the longer chain of the $C_{21}$ additive. The intermolecular bonding analysis (Table 7)

provides further evidence for this: the [001] interaction is decreased on addition of additive showing that the "gap" is in the positive growth direction, the [00-1] interaction is identical with additive present - the additive molecule incorporates perfectly due to its similarity with the host. This is mirrored in the attachment energy results. For both eicosane and heneicosane additives the attachment energy for (00-1) was the same, the value for (001) increases with the chain length. Note that the [001] interaction is -0.15 kcal/mol compared to -0.04 kcal/mol for eicosane (and -0.24 kcal/mol for pure docosane). The additional methylene group in $C_{21}$ results in an increase in this value (compared to eicosane) but because it has a shorter chain length than docosane the value is less than the host-host interaction.

TABLE 6 Changes in incorporation energy (Δb) and attachment energies for docosane with heneicosane additive (in kcal/mol).

| FACE (hkl) | Δb | $E_{att(+)}$'' | $E_{att(-)}$'' | $E_{att}$'' | $E_{att}$ |
|---|---|---|---|---|---|
| (0 0 1) | 1.09 | -1.00 | -1.81 | -2.81 | -3.63 |
| (0 1 0) | 0.91 | -11.78 | -11.15 | -22.93 | -24.04 |
| (0 1 -1) | 0.59 | -12.54 | -11.52 | -24.06 | -25.49 |
| (0 1 1) | 0.94 | -11.62 | -11.73 | -23.35 | -24.42 |
| (0 1 -2) | 0.56 | -12.66 | -11.59 | -24.25 | -25.70 |
| (0 1 2) | 0.58 | -11.83 | -12.36 | -24.19 | -25.62 |
| (0 1 -3) | 0.55 | -12.68 | -11.60 | -24.28 | -25.74 |
| (1 0 3) | 0.64 | -13.54 | -14.63 | -28.17 | -29.73 |
| (1 0 2) | 0.68 | -13.47 | -14.50 | -27.98 | -29.49 |
| (0 1 3) | 0.55 | -11.86 | -12.42 | -24.28 | -25.73 |

TABLE 7 Intermolecular bonding analysis for docosane with heneicosane additive. U, V, W are multiples of the unit cell along the a, b and c-directions, respectively; bond energies are in kcal/mol.

| Bond | U | V | W | Bond Energy Host | Bond Energy Additive |
|---|---|---|---|---|---|
| a | 1 | 0 | 0 | -7.69 | -7.40 |
| b | -1 | 0 | 0 | -7.69 | -7.55 |
| c | 0 | -1 | 0 | -5.87 | -5.63 |
| d | 0 | 1 | 0 | -5.87 | -5.77 |
| e | -1 | 1 | 0 | -3.24 | -3.19 |
| f | 1 | -1 | 0 | -3.24 | -3.10 |
| g | 0 | 0 | 1 | -0.24 | -0.15 |
| h | 0 | 0 | -1 | -0.24 | -0.24 |

Blocker-Type Additives: Docosane With Tricosane As An Additive

The odd numbered n-alkane tricosane ($C_{23}$) was considered to act as a blocker-type additive due to having a longer chain length than the host material. On adsorbing into the docosane lattice, the additive molecule will initially adsorb easily in the c-direction in an identical way to the host molecules (as only methyl-methyl interactions contribute), but the longer chain length will cause large steric interactions on adsorption of subsequent molecules in this direction as the additive is fitting into a space designed for shorter docosane molecules. As a result of this, growth in this direction is expected to be inhibited i.e. the (001) and related faces should have more importance in the morphology. Morphological predictions were obtained using the vacancy approach outlined previously.

The results of the theoretical calculations are given in Table 8, the predicted morphologies in Figures 6(f) and 6(g). It can be seen that the effect of the additive is to decrease the thickness of the crystal slightly, as expected. The values of the attachment energies show the largest decrease to be in the c-direction (due to the vacancy in the [0011] position) and a small increase in the b-direction (due to the extra energy from the extra atoms), the other faces remain relatively unaffected.

The changes in incorporation energy show that additive adsorption in the (001) face is very favourable and that additive molecules can incorporate into all faces with a relatively small degree of energetic loss (all incorporation energy values are less than 1 kcal/mol). For most faces there is little loss of energy due to the small values of the vacancies - the effect of these interactions in a real system would be larger due the accumulative disruption of bonding.

The vacancy energy ($E_V$) was calculated to be 0.05 kcal/mol, with $N_V$=3. $E_V$ is constant for all the blocker additive examples in this paper, although $N_V$ can vary. Table 9 lists the bonds replaced by vacancies along with a detailed intermolecular analysis. Notice how most of the interactions are stronger with the additive present. Again, this results from the extra atoms contributing to the intermolecular interaction. Also note the large blocking effect of the additive along the c-direction (compare this to the disruptive homologues where this value is less than the host due to a shorter chain length, here the longer chain length causes blocking) a vacancy is introduced here as well as in the [-1011] and [0-111] positions: all are adjacent to the central additive molecule. The model 2 morphology also is similar to the host morphology. Here, though, additional {011} faces are observed.

TABLE 8 Changes in incorporation energy (Δb) and attachment energies for docosane with tricosane additive (in kcal/mol).

| FACE (hkl) | Δb | $E_{att(+)}''$ | $E_{att(-)}''$ | $E_{att}''$ | $E_{att}$ |
|---|---|---|---|---|---|
| (0 0 1) | -0.78 | -1.11 | -1.82 | -2.92 | -3.63 |
| (0 1 0) | 0.16 | -12.44 | -12.01 | -24.45 | -24.04 |
| (0 1 -1) | -0.61 | -13.06 | -12.07 | -25.12 | -25.49 |
| (0 1 1) | -0.33 | -11.96 | -12.39 | -24.34 | -24.42 |
| (0 1 -2) | -0.52 | -13.15 | -12.28 | -25.43 | -25.70 |
| (0 1 2) | -0.53 | -12.38 | -12.96 | -25.34 | -25.62 |
| (0 1 -3) | -0.51 | -13.17 | -12.31 | -25.48 | -25.74 |
| (1 0 3) | -0.49 | -14.52 | -15.04 | -29.56 | -29.73 |
| (1 0 2) | -0.55 | -14.33 | -14.93 | -29.26 | -29.49 |
| (0 1 3) | -0.51 | -12.45 | -13.02 | -25.47 | -25.73 |

TABLE 9 Intermolecular bonding analysis for docosane with tricosane additive. U, V, W are multiples of the unit cell along the a, b and c-directions, respectively; bond energies are in kcal/mol. Bonds [-1011] (strength 10.42), [0-111] (strength 2.264) and [0011] (strength 17.28 kcal/mol) were omitted and replaced by vacancies.

| Bond | U | V | W | Bond Energy Host | Additive |
|---|---|---|---|---|---|
| a | 1 | 0 | 0 | -7.69 | -7.93 |
| b | -1 | 0 | 0 | -7.69 | -7.76 |
| c | 0 | -1 | 0 | -5.87 | -5.92 |
| d | 0 | 1 | 0 | -5.87 | -6.05 |
| e | -1 | 1 | 0 | -3.24 | -3.31 |
| f | 1 | -1 | 0 | -3.24 | -3.30 |
| g | 0 | 0 | 1 | -0.24 | 17.28 |
| h | 0 | 0 | -1 | -0.24 | -0.24 |

Blocker-Type Additives: Docosane With Tetracosane As An Additive

The results for tetracosane ($C_{24}$), given in Table 10, are very similar to those obtained for $C_{23}$ with the following exceptions. Since tetracosane has a longer chain again the extra atoms cause an increase in any intermolecular interactions unaffected by steric considerations. The steric effect is even more evident though in the c-direction as host molecules physically overlay the additive and have to be replaced by vacancies ($N_V$=3, see Table 11). The morphologies are shown in Figures 6(h) and 6(i). The large steric effect in the c-direction outweighs any other considerations and

the crystal becomes slightly thinner than those observed with pure host but slightly thicker than with $C_{23}$ as additive. The model 2 crystal (Figure 6(i)) is similar although the {011} and {010} interchange morphological importance.

TABLE 10 Changes in incorporation energy ($\Delta b$) and attachment energies for docosane with tetracosane additive (in kcal/mol).

| FACE (hkl) | $\Delta b$ | $E_{att(+)}''$ | $E_{att(-)}''$ | $E_{att}''$ | $E_{att}$ |
|---|---|---|---|---|---|
| (0 0 1) | -1.26 | -1.53 | -1.82 | -3.35 | -3.63 |
| (0 1 0) | -0.12 | -12.58 | -12.53 | -25.10 | -24.04 |
| (0 1 -1) | -0.88 | -13.14 | -12.65 | -25.78 | -25.49 |
| (0 1 1) | -0.76 | -12.17 | -12.68 | -24.85 | -24.42 |
| (0 1 -2) | -0.73 | -13.23 | -12.92 | -26.15 | -25.70 |
| (0 1 2) | -0.80 | -12.81 | -13.20 | -26.01 | -25.62 |
| (0 1 -3) | -0.72 | -13.24 | -12.96 | -26.20 | -25.74 |
| (1 0 3) | -0.73 | -15.22 | -15.11 | -30.34 | -29.73 |
| (1 0 2) | -0.85 | -14.97 | -15.01 | -29.98 | -29.49 |
| (0 1 3) | -0.73 | -12.94 | -13.25 | -26.19 | -25.73 |

Incorporation energy values show that all faces are susceptible to additive adsorption: all the values are negative with the most likely site being the (001) face which has the most favourable incorporation energy. The least favourable site is the (010) face which is closest to the blocker part of the additive (i.e. the additional two carbons and associated hydrogens). The attachment energy for this face increases on additive addition indicating a decrease in its morphological importance. In fact, comparing $E_{att}''$ (additive) with $E_{att}$ (host) shows that for all faces save (001), $E_{att}''$ is larger than $E_{att}$, implying that the (001) face should increase its morphological importance compared to the pure host system due to the additive blocking oncoming molecules at this face. All other faces should have increased growth (due to larger attachment energies) and therefore decrease in size; the energy changes are very small for the most part so this effect is negligble. These results also indicate that the vacancies have little effect except for the (001) face. This is borne out by the calculated morphologies: the crystal is slightly thinner along c and additional {011} faces appear for the first time in the model 1 morphologies, competing with the now weakened {010} faces.

Comparing the positive and negative components of the additive attachment energies it can be seen that the negative component is more negative for (001), (011), (012), (013) and (102) faces; for the other faces the positive component dominates.

This can be explained by considering the bonding analysis (Table 11) which shows that three vacancies were required - the [0-111] interaction being the most affected by the additive. Note that the c-interaction is only affected in the positive direction - here a vacancy is introduced. The negative interaction is unaffected by the additive. This shows that the extra atoms lie in the +c direction, in the -c direction there is no difference between additive and host molecules. Thus $E_{att(-)}$" dominates over $E_{att(+)}$" for the (001) face. There is very large steric repulsion at the [01-11] site resulting from the blocker part of the additive overlaying this molecule.

TABLE 11 Intermolecular bonding analysis for docosane with tetracosane additive. U, V, W are multiples of the unit cell along the a, b and c-directions, respectively; bond energies are in kcal/mol. Bonds [-1011] (strength 15.62), [0-111] (strength 138.16) and [0011] (strength 33.40 kcal/mol) were omitted and replaced by vacancies.

| Bond | U | V | W | Bond Energy Host | Additive |
|---|---|---|---|---|---|
| a | 1 | 0 | 0 | -7.69 | -8.06 |
| b | -1 | 0 | 0 | -7.69 | -7.80 |
| c | 0 | -1 | 0 | -5.87 | -5.99 |
| d | 0 | 1 | 0 | -5.87 | -6.08 |
| e | -1 | 1 | 0 | -3.24 | -3.32 |
| f | 1 | -1 | 0 | -3.24 | -3.41 |
| g | 0 | 0 | 1 | -0.24 | 33.40 |
| h | 0 | 0 | -1 | -0.24 | -0.24 |

## THE EFFECT OF METHYL-SUBSTITUTED DOCOSANES ON THE MORPHOLOGY OF DOCOSANE

In this section four methyl-substituted docosane derivatives (designated Additives 1-4) are considered as blocker-type additives. Additives 1 and 2 contain a single methyl group on either the first or eleventh carbon of the chain (approximately the chain centre), Additives 3 and 4 have two additional methyl groups placed on the first and eleventh and the first and last carbons of the chain, respectively.

### The Morphology of Docosane in the Presence of Additive 1: 2-Methyl Docosane

The effect of this isoparaffin is much more noticeable than the n-alkane additives considered above. The predicted crystals (Figures 7(b), (c)) are much thicker along the c-axis, less wide along the a-direction and extended along the b-direction. These

observations can be accounted for by examining the results of the energy calculations given in Table 12. $E_{att}''$ is less than $E_{att}$ for all faces by around 2 kcal/mol except for {001} where the difference is only 0.15 kcal/mol and {102} and {103} where the difference is over 10 kcal/mol. For these last two faces the incorporation values are similar to the other faces so it can be expected that the additive will incorporate here but that that the relative morpholgical importance of these faces will increase greatly. This is seen in the Wulff plots.

TABLE 12 Changes in incorporation energy (Δb) and attachment energies for docosane with 2-methyl docosane additive (in kcal/mol).

| FACE (hkl) | Δb | $E_{att(+)}''$ | $E_{att(-)}''$ | $E_{att}''$ | $E_{att}$ |
|---|---|---|---|---|---|
| (0 0 1) | 10.74 | -1.82 | -1.67 | -3.48 | -3.63 |
| (0 1 0) | 7.86 | -12.25 | -8.83 | -21.08 | -24.04 |
| (0 1 -1) | 7.42 | -12.62 | -9.47 | -22.09 | -25.49 |
| (0 1 1) | 7.42 | -12.35 | -8.67 | -21.02 | -24.42 |
| (0 1 -2) | 7.50 | -12.82 | -9.56 | -22.38 | -25.70 |
| (0 1 2) | 7.50 | -12.94 | -9.36 | -22.30 | -25.62 |
| (0 1 -3) | 7.51 | -12.85 | -9.58 | -22.43 | -25.74 |
| (1 0 3) | 7.75 | -4.05 | -14.86 | -18.91 | -29.73 |
| (1 0 2) | 7.65 | -3.95 | -14.63 | -18.57 | -29.49 |
| (0 1 3) | 7.51 | -12.99 | -9.42 | -22.42 | -25.73 |

Since the {102} and {103} forms have dramatically lower attachment energies with additive present they become more morphologically dominant (extending the crystal along along the b- axis) to the detriment of the {010} forms: thus the crystals are less wide. However, the {010} forms still have a similar surface area causing the crystal to become thicker. Note also the considerable difference between the positive and negative components of the {102} and {103} faces. This is due to the asymmetry of the additive with respect to the host molecules.

Additional {011} faces are present in both theoretical habits. When faces are competing in the same zone small changes in growth rates (here represented by attachment energies) can cause the dominance of one over the other, in this case {010} and 011} have closer attachment energies with the additive present.

Regarding the positive and negative components of the additive attachment energies the negative component is always lower (more positive) by around 3-4 kcal/mol except for {001} where the difference is 0.15 kcal/mol and for {102} and {103} where the order changes and the positive components are lower by over 10

kcal/mol causing the polar crystal to increase the size of (102) and (103) at the expense of (-1 0-2) and (-1 0-3).

The incorporation values are all reasonably positive: additive incorporation requires a loss of around 7 kcal/mol for all faces with the (001) face losing around 10 kcal/mol, the least likely surface for adsorption. Therefore a third model of the morphology (Figure 7(d)) has been computed assuming the additive incorporates on all faces save (001). This model shows the expected slight increase in thickness i.e. the {001} forms have increased importance. This is due to the value of $E_{att}$ for (001) being -3.63 kcal/mol compared to -3.48 kcal/mol for $E_{att}$".

TABLE 13 Intermolecular bonding analysis for docosane with 2-methyl docosane additive along the a, b and c-directions, respectively; bond energies are in kcal/mol. Bonds [1-101] (strength 3.80), [10-11] (strength 7.97) and [1001] (strength 0.368 kcal/mol) were omitted and replaced by vacancies.

| Bond | U | V | W | Bond Energy Host | Bond Energy Additive |
|---|---|---|---|---|---|
| a | 1 | 0 | 0 | -7.69 | 0.37 |
| b | -1 | 0 | 0 | -7.69 | -7.78 |
| c | 0 | -1 | 0 | -5.87 | -5.71 |
| d | 0 | 1 | 0 | -5.87 | -5.93 |
| e | -1 | 1 | 0 | -3.24 | -3.27 |
| f | 1 | -1 | 0 | -3.24 | 3.80 |
| g | 0 | 0 | 1 | -0.24 | -0.24 |
| h | 0 | 0 | -1 | -0.24 | -0.30 |

The bonding analysis (Table 13) shows that the strongest host-host interaction between the central molecule and a second molecule removed one unit cell along the positive a direction i.e. [1001] is affected strongly by the additive and is replaced by a vacancy. The corresponding molecule along the negative a direction is not affected however. The b-direction exhibits a similar effect although to a much lesser degree, the -b bond being lowered by 0.16 kcal/mol the +b bond being increased by the same amount due to the contributions of the extra atoms compared to the host molecule. The c-direction is not adversely affected at all: the +c direction loses no energy, the -c direction gains 0.006 kcal/mol. This is because the methyl group is not in the c- plane - it replaces a hydrogen atom in the ab plane. Note how different these results are from those with a $C_{23}$ additive. Although for both $N_V$=3, the methyl group is a much more effective blocker.

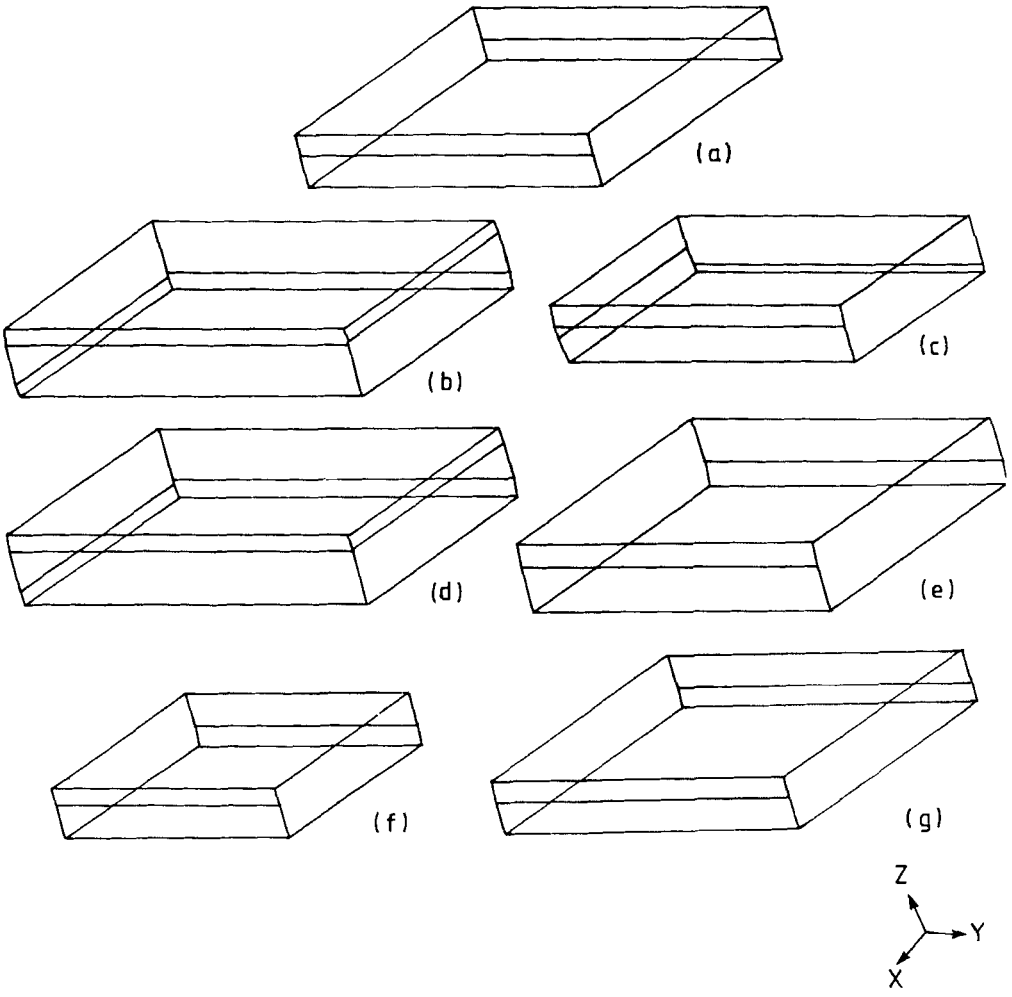


FIGURE 7 Habit modification of docosane by methyl-substituted docosanes: (a) attachment energy morphology of docosane; (b) with 2-methyl docosane (model 1); (c) with 2-methyl docosane (model 2); (d) with 2-methyl docosane (model 3); (e) with 11-methyl docosane (model 1); (f) with 11-methyl docosane (model 2); (g) with 11-methyl docosane (model 3). Faces additional to those shown in Figure 5 are {011}.

The Morphology of Docosane in the Presence of Additive 2: 11-Methyl Docosane

The effect of this additive is clearly illustrated in Figure 7(e). This model 1 crystal is thicker again in the c-direction than with Additive 1, although it is not extended along the b-direction and no {011} forms are predicted. The crystals exhibit the same faces as docosane but the reduction in growth rate of the a and b-directions is clear from the aspect ratio of the crystal.

The energy results given in Table 14 show that the attachment energies with additive present are of much lower magnitude than for docosane, probably due to the vacancies ($N_V$=2), except for {001} where $E_{att}$" is virtually identical to $E_{att}$. Since the other forms have smaller attachment energies than in the host system, they increase in size relative to the {001} faces which explains the predicted morphology. Note how the (001) attachment energy is almost unchanged by additive adsorption. This is a result of the extra methyl group being in the middle of the molecule and no longer in the c-direction. Here it interacts with the a and b directions whilst the end chain interactions are almost completely unaffected by its presence. This is also reflected in the fact that the positive and negative components of $E_{att}$" are of equal magnitude for this face, since there is no difference between chain ends. Contrast this to the effect of Additive 1 (with the methyl group at the end of the chain) where $E_{att}$" for (001) is lowered by the additive and the positive and negative components were different due to the additive asymmetry with respect to this face.

The positive and negative components of the additive attachment energies for the other faces demonstrates the asymmetry of the additive and the polarity it induces. There is a disparity of about 5 kcal/mol, increasing to 7 kcal/mol for the {102} and {103} forms. The negative component is consistently the larger (more negative) of the two, indicating that the methyl group protrudes into the positive growth direction. Despite this the polar crystal (Figure 7(f)) is almost identical to Figure 7(e).

The bonding analysis (Table 15) further demonstrates this effect. Both c-direction bonds are indentical both to each other and to the pure host-host interaction: only the end methyl groups are interacting here and they remain unaffected by the methyl on the middle carbon. Conversely, the asymmetry is shown by all the other intermolecular interactions. The positive a-direction bond and the positive b-direction bond interact strongly with the protruding methyl group and require to be replaced by vacancies confirming the lowering of the positive additive attachment energies.

The incorporation values are uniformly the same with the exceptions of the {103}

and {102} forms, which are differ only slightly, and of the {001} forms, this time the most favoured faces for additive adsorption (for Additive 1 they were the least favoured - this is probably a result of the end methyl interactions being unchanged with Additive 2 present). This indicates the possibility that the additive adsorbs only on the {001} faces with all other faces unaffected due to having higher Δb values. Such an effect was calculated using $E_{att}''$ for {001} and $E_{att}$ (i.e. host) values for the other faces. This model is shown in Figure 7(g). The morphology is more-or-less identical to the host crystal since for (001) $E_{att}''$ is -3.64 kcal/mol and $E_{att}$ is -3.63 kcal/mol.

TABLE 14 Changes in incorporation energy (Δb) and attachment energies for docosane with 11-methyl docosane additive (in kcal/mol).

| FACE (hkl) | Δb | $E_{att(+)}''$ | $E_{att(-)}''$ | $E_{att}''$ | $E_{att}$ |
|---|---|---|---|---|---|
| (0 0 1) | 12.74 | -1.82 | -1.82 | -3.64 | -3.63 |
| (0 1 0) | 13.41 | -6.63 | -12.22 | -18.84 | -24.04 |
| (0 1 -1) | 13.41 | -7.35 | -12.94 | -20.29 | -25.49 |
| (0 1 1) | 13.41 | -6.82 | -12.41 | -19.23 | -24.42 |
| (0 1 -2) | 13.41 | -7.46 | -13.05 | -20.51 | -25.70 |
| (0 1 2) | 13.41 | -7.42 | -13.01 | -20.43 | -25.62 |
| (0 1 -3) | 13.41 | -7.48 | -13.07 | -20.55 | -25.74 |
| (1 0 3) | 13.48 | -7.57 | -15.22 | -22.79 | -29.73 |
| (1 0 2) | 13.48 | -7.45 | -15.10 | -22.55 | -29.49 |
| (0 1 3) | 13.41 | -7.47 | -13.06 | -20.54 | -25.73 |

TABLE 15 Intermolecular bonding analysis for docosane with 11-methyl docosane additive. U, V, W are multiples of the unit cell along the a, b and c-directions, respectively; bond energies are in kcal/mol. Bonds [0101] (strength 0.232) and [1001] (strength 11.43 kcal/mol) were omitted and replaced by vacancies.

| Bond | U | V | W | Bond Energy Host | Additive |
|---|---|---|---|---|---|
| a | 1 | 0 | 0 | -7.69 | 11.43 |
| b | -1 | 0 | 0 | -7.69 | -7.78 |
| c | 0 | -1 | 0 | -5.87 | -5.92 |
| d | 0 | 1 | 0 | -5.87 | 0.23 |
| e | -1 | 1 | 0 | -3.24 | -3.43 |
| f | 1 | -1 | 0 | -3.24 | -3.33 |
| g | 0 | 0 | 1 | -0.24 | -0.24 |
| h | 0 | 0 | -1 | -0.24 | -0.24 |

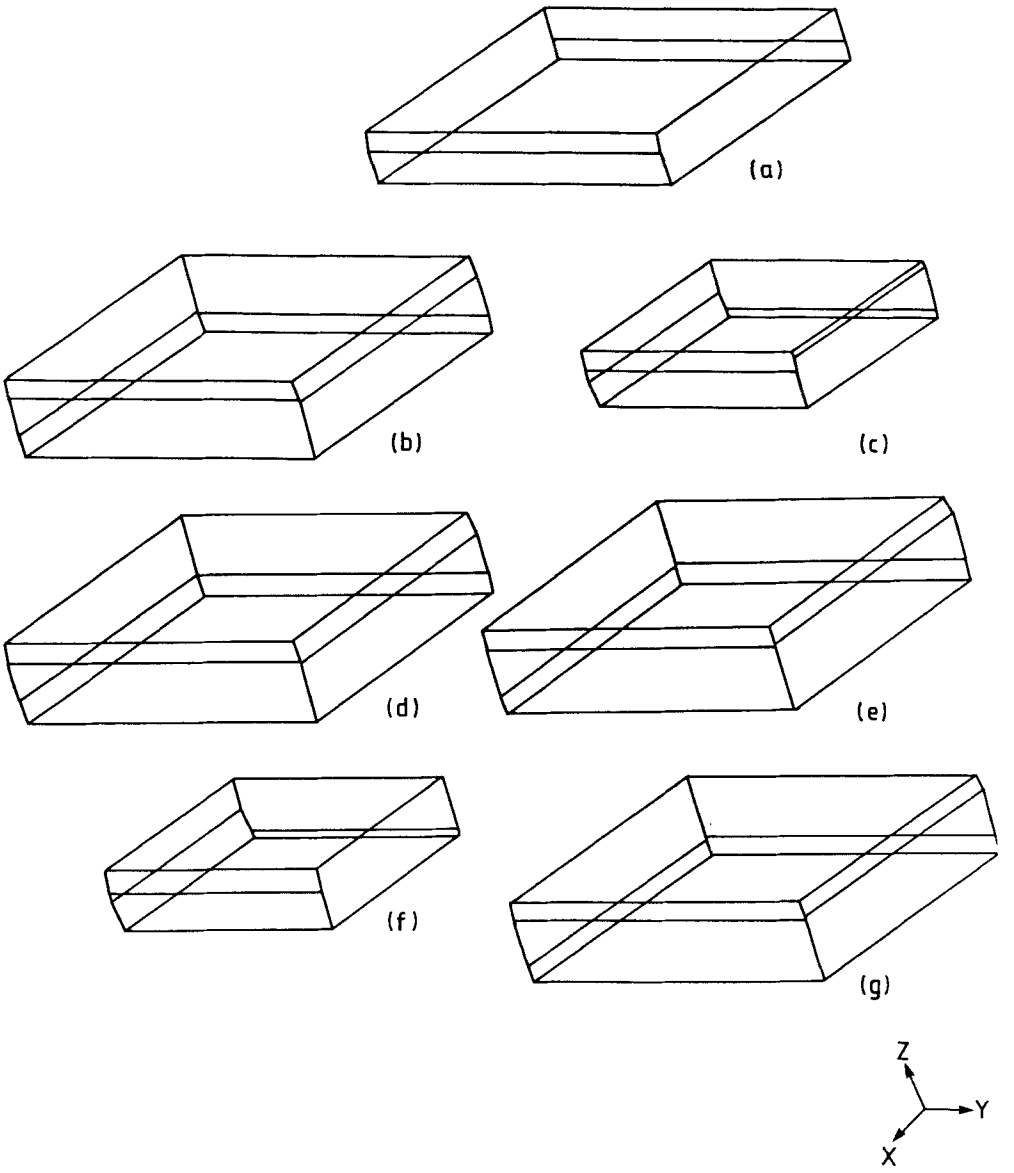


FIGURE 8 Habit modification of docosane by dimethyl-substituted docosanes: (a) attachment energy morphology of docosane; (b) with 2,11-dimethyl docosane (model 1); (c) with 2,11- dimethyl docosane (model 2); (d) with 2,11-dimethyl docosane (model 3); (e) with 2,21-dimethyl docosane (model 1); (f) with 2,21-dimethyl docosane (model 2); (g) with 2,21-dimethyl docosane (model 3). Faces additional to those shown in Figure 5 are {011}.

The Morphology of Docosane in the Presence of Additive 3: 2, 11-Dimethyl Docosane

The effect of 2,11-dimethyl docosane as an additive is shown in Figure 8(b). It has a similar but more pronounced morphological effect than Additive 2. A much thicker and less platy crystal containing {011} faces is produced. This is due to the additional methyl groups on the additive causing steric interactions in the a and b-planes ($N_V$=4) which in turn result in an inhibition of growth along these directions.

The asymmetry caused by the methyl groups causes the magnitude of $E_{att(+)}$" and $E_{att(-)}$" to differ and the resulting crystal (Figure 8(c)) to be very polar with respect to the {011} faces, though less so with the {102} and {103} faces.

On examing the energy results given in Table 16 in detail, it can be seen that the incorporation values are very positive implying that any additive adsorption is reasonably hard. The largest value is for the (001) face implying it is the least likely site for adsorption, the others are all slightly less with the (010), (103) and (102) faces the next least likely sites as in the previous example. This illustrates the need for a further morphological prediction (model 3) using $E_{att}$" for all faces except for {001} which is given the host attachment energy value (i.e. assuming no additive incorporation here). This model (Figure 8(d)) shows a habit very similar to, but slightly thicker than the model 1 morphology since $E_{att}$" is more negative than the corresponding value of $E_{att}$ (-3.49 kcal/mol compared to -3.63 kcal/mol).

The $E_{att}$" values are around 8.5 kcal/mol more positive than the corresponding $E_{att}$ values except for {102} and {103} which are around 10 kcal/mol more positive (probably due to vacancies) and {001} which is 0.14 kcal/mol less negative (due to the methyl group being out of the c- plane, see below).

The negative growth components of the additive attachment energies are larger than the positive components by around 2.5 kcal/mol except for {001} where the order reverses and the positive component is 0.15 kcal/mol larger, and for {103}, {102} which are over 11 kcal/mol more negative in favour of the negative component. The $E_{att(-)}$" values have the larger attachment energies as the methyl groups protrude into the positive growth direction. This is due to the asymmetry of the additive with respect to the host molecules (one end of the molecule having no extra methyl groups) causing the polar crystal to increase the size of (102) and (103) at the expense of (-1 0-2) and (-1 0-3). The order reverses for {001} as one end has no additional methyl groups and therefore the attachment energy here is unchanged compared to the host system (cf. Additive 1), at the other end there are more atoms

giving rise to a more negative attachment energy.

The bonding analysis (Table 17) shows four vacancies, the most sterically affected is the positive a-direction bond. This shows that methyl groups in the middle of the chain have a greater steric effect as here the intermolecular interactions are greater than in the c-direction (cf. Figure 1). Thus the positive b-bond is also



TABLE 16 Changes in incorporation energy (Δb) and attachment energies for docosane with 2, 11-dimethyl docosane additive (in kcal/mol).

| FACE (hkl) | Δb | $E_{att(+)}''$ | $E_{att(-)}''$ | $E_{att}''$ | $E_{att}$ |
|---|---|---|---|---|---|
| (0 0 1) | 15.94 | -1.82 | -1.67 | -3.49 | -3.63 |
| (0 1 0) | 13.64 | -6.79 | -8.94 | -15.73 | -24.04 |
| (0 1 -1) | 13.20 | -7.16 | -9.57 | -16.74 | -25.49 |
| (0 1 1) | 13.20 | -6.89 | -8.78 | -15.67 | -24.42 |
| (0 1 -2) | 13.28 | -7.36 | -9.67 | -17.03 | -25.70 |
| (0 1 2) | 13.28 | -7.49 | -9.47 | -16.96 | -25.62 |
| (0 1 -3) | 13.29 | -7.39 | -9.69 | -17.08 | -25.74 |
| (1 0 3) | 13.61 | -4.35 | -15.22 | -19.57 | -29.73 |
| (1 0 2) | 13.51 | -4.25 | -14.98 | -19.23 | -29.49 |
| (0 1 3) | 13.29 | -7.54 | -9.53 | -17.07 | -25.73 |

TABLE 17 Intermolecular bonding analysis for docosane with 2, 11-dimethyl docosane additive. U, V, W are multiples of the unit cell along the a, b and c-directions, respectively; bond energies are in kcal/mol. Bonds [0101] (strength 0.172), [1-101] (strength 3.71), [10-11] (strength 7.98) and [1001] (strength 19.49 kcal/mol) were omitted and replaced by vacancies.

| Bond | U | V | W | Bond Energy Host | Bond Energy Additive |
|---|---|---|---|---|---|
| a | 1 | 0 | 0 | -7.69 | 19.49 |
| b | -1 | 0 | 0 | -7.69 | -7.87 |
| c | 0 | -1 | 0 | -5.87 | -5.76 |
| d | 0 | 1 | 0 | -5.87 | 0.17 |
| e | -1 | 1 | 0 | -3.24 | -3.46 |
| f | 1 | -1 | 0 | -3.24 | 3.71 |
| g | 0 | 0 | 1 | -0.24 | -0.24 |
| h | 0 | 0 | -1 | -0.24 | -0.30 |

affected but the c-bonds are not as the methyl groups are not directly in the c-plane as the extra methyl groups in the $C_{23}$ and $C_{24}$ examples were. In those cases the appropriate c interaction was replaced by a vacancy due to the steric repulsion, whereas for methyl groups added to the adjacent carbon (Additives 1 and 2) the [001] interactions were not affected. The latter effect is also appropriate here.

All the other bonds (save those replaced by vacancies) show the additive values to be larger than the host except the negative b-bond which is slightly smaller (probably related to the corresponding positive direction bond being sterically hindered). This clearly illustrates the polar nature of the bonding with the additive present.



The Morphology of Docosane in the Presence of Additive 4: 2, 21-Dimethyl Docosane

As with all the other methyl-substituted additives the predicted crystals with additive present (Figures 8(e),(f)) exhibit a different combination of forms than docosane itself. The predicted crystals are considerably thicker in the c-direction than any of the previous examples and are also much shortened in the a and b-directions. The overall effect is to modify the long plate-like crystals of docosane to produce a tabular habit, in fact, the most block-like of all the examples in this paper. For both di-methyl docosanes (Additives 3 and 4) $N_V$=4, for the other examples less vacancies are formed, showing that $N_V$ is a useful indication of blocking ability.

The energy results are given in Table 18. The incorporation values are similar to Additive 3: it seems that the di-substituted paraffins are harder to accomodate. {001} has the largest $\Delta b$ and is therefore the least likely site for incorporation. Correspondingly, a third model of the morphology was computed considering the additive adsorbing onto all faces save (001). The habit (shown in Figure 8(g)) is slightly thinner than before because the attachment energy used for (001) is now -3.63 kcal/mol (the value of $E_{att}$) as opposed to -3.77 kcal/mol (the value of $E_{att}$") i.e. a lower attachment energy therefore more morphologically important. The other least-favoured sites are as before: {010}, {102} and {103}.

$E_{att}$" is less than $E_{att}$ for all faces by the same amounts as in the previous example (Additive 3). This indicates that both di-methyl substituted docosanes are of similar blocking ability.

The values of $E_{att(+)}$" and $E_{att(-)}$" also demonstrate similar results to Additive 3 - only for {001} is the negative component dominant. Again {102} and {103} exhibit the greatest disparity. This is because for these faces the asymmetry is the greatest.

The bonding analysis (Table 19) shows the same vacancy pattern as Additive 3. But note the values for the c-direction bonds [001] and [00-1]. In this case both additive bonds are increased on addition of additive whereas only the negative c-bond was increased for Additive 3. This is due to Additive 4 having methyl groups at both ends of the molecule: Additive 3 is a very asymmetric molecule; Additive 4 is much more symmetrical.

TABLE 18 Changes in incorporation energy (Δb) and attachment energies for docosane with 2, 21-dimethyl docosane additive (in kcal/mol).

| FACE (hkl) | Δb | $E_{att(+)}$'' | $E_{att(-)}$'' | $E_{att}$'' | $E_{att}$ |
|---|---|---|---|---|---|
| (0 0 1) | 16.12 | -2.10 | -1.67 | -3.77 | -3.63 |
| (0 1 0) | 13.53 | -6.74 | -8.98 | -15.72 | -24.04 |
| (0 1 -1) | 13.19 | -7.06 | -9.77 | -16.83 | -25.49 |
| (0 1 1) | 13.19 | -7.00 | -8.76 | -15.76 | -24.42 |
| (0 1 -2) | 13.32 | -7.25 | -9.92 | -17.17 | -25.70 |
| (0 1 2) | 13.32 | -7.65 | -9.44 | -17.09 | -25.62 |
| (0 1 -3) | 13.33 | -7.28 | -9.95 | -17.22 | -25.74 |
| (1 0 3) | 13.62 | -4.60 | -15.08 | -19.68 | -29.73 |
| (1 0 2) | 13.51 | -4.48 | -14.85 | -19.33 | -29.49 |
| (0 1 3) | 13.33 | -7.71 | -9.51 | -17.21 | -25.73 |

TABLE 19 Intermolecular bonding analysis for docosane with 2, 21-dimethyl docosane additive. U, V, W are multiples of the unit cell along the a, b and c-directions, respectively; bond energies are in kcal/mol. Bonds [0101] (strength 0.153), [1-101] (strength 3.73), [10-11] (strength 7.97), [1001] (strength 19.39 kcal/mol) were omitted and replaced by vacanies.

| Bond | U | V | W | Bond Energy Host | Bond Energy Additive |
|---|---|---|---|---|---|
| a | 1 | 0 | 0 | -7.69 | 19.39 |
| b | -1 | 0 | 0 | -7.69 | -7.83 |
| c | 0 | -1 | 0 | -5.87 | -5.75 |
| d | 0 | 1 | 0 | -5.87 | 0.15 |
| e | -1 | 1 | 0 | -3.24 | -3.39 |
| f | 1 | -1 | 0 | -3.24 | 3.73 |
| g | 0 | 0 | 1 | -0.24 | -0.29 |
| h | 0 | 0 | -1 | -0.24 | -0.30 |

In this example the methyl groups are on the first and last carbons of the docosane chain. Such an additive has a reasonable effect on the morphology To increase this

effect a larger side group, perhaps a phenyl ring, could be introduced to produce a non tailor-made additive of the blocking type. It is important to note that this type of additive still has to exhibit similar structural features to enable incorporation into the host lattice.



## SUMMARY AND CONCLUSIONS

We have presented a comprehensive approach for modelling the morphology of molecular crystal is the presence of tailor-made additives of the disruptor and blocker types and demonstrated this approach through a detailed study examining the mediation of the morphlogy of docosane by the presence of with eight tailor-made additive molecules based on docosane.

The results showed that calculations of the incorporation energy as a function of additive provides a useful bench-mark for assessing whether an additive will incorporate on a surface and if so whether it will uniformly incorporate.

The structural parameter $E_{att}$" was introduced to enable calculation of the relative growth rate of the morphological forms as a function of additive incorporation and hence simulation of the morphology of the habit-modified crystals. It was successfully modified to enable more meaningful calculations on blocker-type additives to be obtained by replacing unfavourable steric repulsions encountered as a result of the blocking nature of the additive with vacancies thus lowering the attachment energies for faces which are "blocked", simulating the slower growth and allowing direct prediction of morphologies.

Attention is drawn to the polar effect on introduction of additives which this approach also models. The polar crystals exhibit certain faces (hkl) without corresponding (-h-k-l) forms. By breaking the symmetry the additive greatly affects the relative growth rates of these pairs of faces.

Considering the four n-alkane homologues as additives demonstrates the ability of these materials to incorporate easily into docosane crystals. The habit-modifying properties are not great due to the similarity with the host sytem and the anisotropic nature of the bonding. The predicted crystals are always thinner along the c-direction than the pure system (the attachment energy for the (001) face is always decreased compared to docosane), although they increase in thickness with chain length from n=20-24. Both disruptors and blockers achieve the same morphological result but by

different mechanisms: the former reduce the (001) attachment energy by by reducing the effect of methyl-methyl interactions across the (001) basal plane; the latter block the (001) face causing slower growth in this direction.

Addition of methyl groups to n-alkanes can have a significant effect on their morphology. The similarity with the host molecules allows them to bind to the surface where blocking procedures occur due to the methyl groups interacting adversely with oncoming host molecules. Such effects are most pronounced with di-substituted n-alkanes. More equant crystals are produced going from 2-methyl to 11-methyl to 2, 11 di-methyl to 2, 21 di-methyl docosane as additives.

The overall schematic presented here in the case of tailor-made additives has also been applied to the case of polar morphology[37] and solvent adsorption[38,39]. Work is currently in progress to model the case of additives which are not "tailor-made"; this work will be presented in a future paper.

## ACKNOWLEDGEMENTS

This work has been supported, in part, through research grants from SERC and Exxon Chemical to whom we are grateful for financial support of a research assistantship (GC[40]) and a senior fellowship (KJR).

## APPENDIX: LIST OF SYMBOLS

| | |
|---|---|
| (hkl) | Miller indices of crystal growth face |
| {hkl} | Miller indices of symmetry-equivalent crystal growth faces |
| $d_{hkl}$ | interplanar spacing for face (hkl) thus slice thickness of growth slice (hkl) |
| $E_{cr}$ | lattice (or crystallisation) energy of crystal |
| $E_{sl}$ | slice energy of growth slice (hkl) |
| $E_{att}$ | attachment energy of growth slice (hkl), sum of $E_{att(+)}$ and $E_{att(-)}$ |
| $E_{att(+)}$ | attachment energy of growth slice (hkl) along the positive growth direction for pure system (equal to $E_{att(-)}$) |

| | |
|---|---|
| $E_{att(-)}$ | attachment energy of growth slice (hkl) along the negative growth direction for pure system (equal to $E_{att(+)}$) |
| U, V, W | multiples of the unit cell along the crystal directions a, b and c |
| Z | position of symmetry-related molecule in the unit cell |
| $E_{sl'}$ | slice energy with additive at centre of growth slice (hkl) |
| $E_{att'}$ | attachment energy of growth slice (hkl) containing additive onto pure surface (sum of $E_{att(+)'}$ and $E_{att(-)'}$) |
| $E_{att(+)'}$ | attachment energy of growth slice (hkl) containing additive onto pure surface in positive growth direction |
| $E_{att(-)'}$ | attachment energy of growth slice (hkl) containing additive onto pure surface in negative growth direction |
| $E_{att''}$ | attachment energy of pure growth slice (hkl) onto surface containing additive (sum of $E_{att(+)''}$ and $E_{att(-)''}$) |
| $E_{att(+)''}$ | attachment energy of pure growth slice (hkl) onto surface containing additive in positive growth direction |
| $E_{att(-)''}$ | attachment energy of pure growth slice (hkl) onto surface containing additive in negative growth direction |
| $E_b$ | incorporation energy of pure material (equals $E_{sl} + E_{att}$) |
| $E_{b'}$ | incorporation energy of additive (equals $E_{sl'} + E_{att'}$) |
| $\Delta b$ | difference in incorporation energy (equals $E_{b'} - E_b$) |
| $E_v$ | un-relaxed vacancy formation energy |
| $E_{vac(ij)}$ | lattice energy with vacancy at molecular site i, summation commencing from central molecule Z=j |
| $N_m$ | number of molecules in atom-atom summation sphere |
| $N_v$ | number of vacancies generated by blocking additive |
| $R_{lim}$ | limiting radius of atom-atom summation sphere |

## REFERENCES


1. A. Bravais, Etudes Crystallographiques (Paris, 1913)
2. G. Friedel, Bull. Soc. Franc. Mineral. 30 (1907) 326
3. J.D.H. Donnay and D. Harker, Amer. Mineralogist 22 (1937) 463
4. P. Hartman and W.G. Perdok, Acta Cryst. 8 (1955) 49
5. P. Hartman and W.G. Perdok, Acta Cryst. 8 (1955) 521
6. Z. Berkovitch-Yellin, J. Amer. Chem. Soc. 107 (1985) 8239
7. G. Clydesdale, K.J. Roberts, R. Docherty (submitted to J. Crystal Growth)
8. G. Clydesdale, K.J. Roberts, K. Lewtas, R. Docherty (submitted to J. Crystal Growth)
9. K.J. Roberts, J.N. Sherwood and A. Stewart, J. Crystal Growth 102 (1990) 419
10. A. Gerson, K.J. Roberts and J.N. Sherwood, Acta Cryst. B47 (1991) 280
11. H. Luth, S.C. Nyburg, P.M. Robinson, H.G. Scott, Mol. Cryst. Liq. Cryst. 22 (1974) 337
12. P. Hartman and P. Bennema, J. Crystal Growth 49 (1980) 145
13. H.J. Human, J.P. van der Eerden, L.A.M.J. Jetten and J.G.M. Oderkerken, J. Crystal Growth 51 (1981) 589
14. W.C. Mackrodt, R.J. Davey, S.N. Black and R. Docherty, J. Crystal Growth 80 (1987) 441
15. R. Docherty and K.J. Roberts, J. Crystal Growth 88 (1988) 159
16. D. E. Williams - PCK83, Program No. 481, QCPE Bulletin 4(3) (1983) 82, Quantum Chemistry Program Exchange
17. R. Buckingham and J. Corner, Proc. Royal. Soc. London 189 (1947) 118
18. D.E. Williams, J. Phys. Chem. 45 (1966) 3370
19. G. Clydesdale and K.J. Roberts, in Particle Design via Crystallisation (Eds. R. Ramanarayanan, W. Kern, M. Larson and S. Sikdar), Amer Inst Chem Eng Symp Ser 284 87 (1991) 130
20. R. Docherty, K.J. Roberts and E. Dowty, Comp. Phys. Communications 51 (1988) 423
21. G. Clydesdale, R. Docherty and K.J. Roberts, Comp. Phys. Communications 64 (1991) 311
22. CERIUS molecular modelling software for materials research from Molecular Simulations Inc. of Burlington, MA, and Cambridge, UK.
23. G. Wulff, Z. Kristallogr. 34 (1901) 499
24. M. Lahav, Z. Berkovitch-Yellin, J. van Mil, L. Addadi, M. Idelson and L. Leiserowitz, Isr. J. Chem. 25 (1985) 353
25. HABIT93 - G. Clydesdale, R. Docherty and K. J. Roberts, to be submitted to Comp. Phys. Communications.
26. R. Docherty Modelling the Morphology of Molecular Crystals, PhD Thesis (University of Strathclyde, Glasgow, 1989)
27. L. Addadi, Z. Berkovitch-Yellin, I. Weissbuch, M. Lahav and L. Leiserowitz, Topics In Stereochemistry 16 (1986) 1-85

28. CSSR - Crystal Structure Search Retrieval Database, SERC Chemical Databank System, CSE Applications Group, Daresbury Laboratory, Warrington, England
29. CHEM-X, developed and distributed by Chemical Design Ltd., Oxford, England
30. INTERCHEM. R. Breckinridge and P. Bladon, University of Strathclyde, Glasgow, Scotland (1989)
31. S. C. Nyburg and J. A. Potworowski, Acta Cryst. B29 (1973) 347
32. S.C. Nyburg and H. Lüth, Acta Cryst. B28 (1972) 2992
33. J.D. Cox and G. Pilchard, Thermochemistry of Organic and Organometallic Compounds (Academic Press, New York, 1970)
34. K. Lewtas, D. H. M. Beiny, J. W. Mullin, J. Crystal Growth 102 (1990) 801
35. K. Lewtas, R. D. Tack, D. H. M. Beiny, J. W. Mullin in: Advances In Industrial Crystallisation, eds. J. Garside, R. J. Davey and A. G. Jones (Butterworth-Heimann, 1991) p 166
36. K. Lewtas (unpublished results)
37. R. Docherty, K.J. Roberts, V. Saunders, S. Black and R.J. Davey, J. Chem. Soc. Faraday Disc. 95 (1993) in press
38. K.J. Roberts, J.N. Sherwood, C.S. Yoon and R. Docherty, to be submitted to J. Crystal Growth
39. K.J. Roberts, R. Docherty, P. Bennema and L.A.M.J. Jetten, J. Phys. D: Applied Physics 26B (1993) 7
40. G. Clydesdale, The Development o Predictive Approaches for Modelling the Polymorphic Stability and Crystal Habit of Normal Alkanes and Other Molecular Crystals, Ph.D. Thesis, University of Strathclyde, Glasgow, 1991